EQUIVALENT DC IMPEDANCE OF A THREE-PHASE IMPEDANCE THROUGH AN INVERTER

Quentin DELHAYE
MEED,iMMC (UCLouvain) – Belgium
q.delhaye@uclouvain.be

Marc BEKEMANS
MEED,iMMC (UCLouvain)– Belgium
marc.bekemans@uclouvain.be

Emmanuel DE JAEGER
MEED,iMMC (UCLouvain) - Belgium
emmanuel.dejaeger@uclouvain.be

ABSTRACT

The distribution grid is currently changing. The number of inverters interfacing Low and Medium voltage DC systems has been gradually increasing. The same rectifiers/inverters are also converting the DC voltage, produced by Photovoltaic panels (PVs), into AC voltages (the distribution system, e.g.). Moreover, some DC microgrids need AC/DC converter to have a link with the main grid. This work aims to study and understand the impact of the three-phase (AC) network impedance on the DC side of an AC/DC converter. To do so, the AC impedance is translated into the DC side of the converter through an equivalent DC impedance. This DC equivalent impedance depends on the PWM parameters (modulating index, e.g.). Therefore, this DC equivalent impedance can be used by the upper control layers (i.e. current controls, power controls). The behaviour of the equivalent model in DC as a resistive-inductive load will be presented. The mathematical development is implemented in MATLAB/Simulink and the simulation results are verified through an experimental implementation. Based on these results, the performance of this DC equivalent electrical circuit model will be studied along with some improvements possible on this model.

INTRODUCTION

Historically, Tesla won the War of Currents in the late 1880s. The Alternating Current (AC) was introduced in the energy sector [1]. Nowadays, DC technology is gaining new insights in the energy sector. Photovoltaic panels are emerging on the distribution grid leading to the creation of a new category of grid actors: the ‘prosumers’. Moreover, DC microgrids are emerging with the use of energy storages, electric vehicles (EV’s) or LED lights which are DC technologies [2]. In addition, working directly in DC offers a higher efficiency due to the decreasing number of conversion stages (less inverters or rectifiers involved). Even if DC microgrids tend to operate in an isolated manner, the non-isolated ones are still connected to the main grid through an inverter (AC/DC converter). Therefore, it is important to know the impact of this converter on the DC side considering the behaviour of the AC grid.

To know accurately the behaviour of the converter, different methods exist. These methods are the switching model and the averaged model. The switching model has the advantage of providing accurate results but it is not practical to use in a large-scale environment as it takes a high computational time. On the other hand, the averaged model represents the average value of the switching model. This model is useful to illustrate the main behaviour of the converter. However, this average model has two decoupled parts: AC and DC as show in Fig.1.

In this work, an ‘unified’ averaged model is a target. The

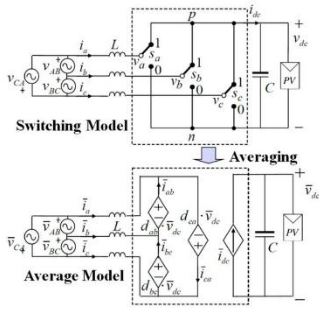

Figure 1: Actual modeling of the averaged model inverter [3]

goal is to find the equivalent DC impedance of an AC impedance through an inverter by transferring the AC impedance to the DC side. This unified DC circuit allows further investigations on the stability of the system using Lyapunov theories, e.g. Moreover, the modeling is using the low-level control parameters such as the modulating index or the phase of the PWM controlling the converter. Doing so, the model presented in this work is not influenced by the type of the upper controls (current/power controllers).

First, the mathematical modeling development is computed. Then, based on this mathematical model, the electrical modeling is performed. After the theoretical part, results from simulations on MATLAB/Simulink and experiments are shown. At the end, a conclusion is drawn.

MODELING OF THE DC-EQUIVALENT IMPEDANCE

The global methodology is illustrated. Then, the DC-equivalent impedance expression is computed mathematically. These results are useful to develop the electrical model proposed in the following section: circuit modeling of the DC equivalent impedance.

Methodology used

The methodology used is the following (Fig.2).

Step 1: Introduction of a voltage source on the DC side a voltage source on the DC side, consisting of a DC component and an AC perturbation.

Step 2: Computation of the three-phase voltages resulting from the voltage source introduced at Step 1.

Step 3: Based on the AC circuit impedance, the phase currents are computed using the phase voltages found in Step 2.

Step 4: The current flowing in the DC line is computed thanks to the three-phase currents from Step 3.

A three-phase PWM (with m, the modulation index and ω_e, the frequency of the modulating wave and ϕ, the phase) is used to control the AC-DC inverter.

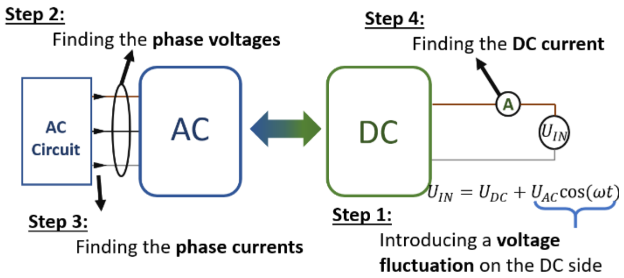

Figure 2 Schematic representation of the method used

Each step has an important element linked to it:

- U_{IN}, the input DC voltage with an AC perturbation part (introducing the perturbation pulsation, ω,see Fig. 2) (Step 1)
- the AC/DC inverter (modulates the DC signals to ω_e frequency) (Step 2)
- Z_{AC}, the AC circuit impedance to be analyzed (Step 3)
- A, the amperemeter to measure the DC current resulting from modulating back the AC three-phase currents to the DC side (Step 4)

The mathematical development corresponding to these steps is detailed in the next section.

Mathematical development

The DC voltage source is (Step 1):

$$U_{IN} = U_{DC} + U_{AC}\, cos(\omega t) \qquad (1)$$

Then, the inverter brings the DC voltage (U_{IN}) to the ω_e pulsation (Step 2). This is the conversion step from DC to AC.

$$U_{3AC} := \begin{cases} U_a = \alpha U_{IN}\cos(\omega_e t + \phi) \\ U_b = \alpha U_{IN}\cos\left(\omega_e t + \dfrac{2\pi}{3} + \phi\right) \\ U_c = \alpha U_{IN}\cos\left(\omega_e t - \dfrac{2\pi}{3} + \phi\right) \end{cases} \qquad (2)$$

where α ($=\frac{m}{2}$) is half the modulating index, and ϕ, the phase of the PWM modulating wave.
Without any loss of generality, the mathematical development will focus on phase B (U_b). In polar form, U_b can be written as:

$$\begin{aligned} U_b &= \frac{\alpha\, U_{DC} e^{j\left(\omega_e t + \frac{2\pi}{3} + \phi\right)}}{2} + \frac{\alpha\, U_{DC} e^{j\left(-\omega_e t - \frac{2\pi}{3} - \phi\right)}}{2} \\ &+ \frac{\alpha\, U_{AC} e^{j\left((\omega_e+\omega)t + \frac{2\pi}{3} + \phi\right)}}{4} + \frac{\alpha\, U_{AC} e^{j\left((-\omega_e+\omega)t - \frac{2\pi}{3} - \phi\right)}}{4} \\ &+ \frac{\alpha\, U_{AC} e^{j\left((\omega_e-\omega)t + \frac{2\pi}{3} + \phi\right)}}{4} + \frac{\alpha\, U_{AC} e^{j\left((-\omega_e-\omega)t - \frac{2\pi}{3} - \phi\right)}}{4} \end{aligned} \qquad (3)$$

Dividing this phase voltage by the impedance results in the phase current (I_b) flowing through the AC impedance ($\bar{Z}(\omega)$) (Step 3) as shown in (4).
By analogy, phase A and C currents can be found.

$$\begin{aligned} I_b = \frac{U_b}{Z_b} &= \frac{\alpha\, U_{DC} e^{j\left(\omega_e t + \frac{2\pi}{3} + \phi\right)}}{2\bar{Z}(\omega_e)} + \frac{\alpha\, U_{DC} e^{j\left(-\omega_e t - \frac{2\pi}{3} - \phi\right)}}{2\bar{Z}(-\omega_e)} \\ &+ \frac{\alpha\, U_{AC} e^{j\left((\omega_e+\omega)t + \frac{2\pi}{3} + \phi\right)}}{4\bar{Z}(\omega_e+\omega)} + \frac{\alpha\, U_{AC} e^{j\left((-\omega_e+\omega)t - \frac{2\pi}{3} - \phi\right)}}{4\bar{Z}(-\omega_e+\omega)} \\ &+ \frac{\alpha\, U_{AC} e^{j\left((\omega_e-\omega)t + \frac{2\pi}{3} + \phi\right)}}{4\bar{Z}(\omega_e-\omega)} + \frac{\alpha\, U_{AC} e^{j\left((-\omega_e-\omega)t - \frac{2\pi}{3} - \phi\right)}}{4\bar{Z}(-\omega_e-\omega)} \end{aligned} \qquad (4)$$

Using the property of complex numbers (for any c),

$$c + c^* = 2\,\Re(c)$$

(4) can be rewritten as:

$$\begin{aligned} I_b &= \alpha U_{AC} \frac{\cos\left((\omega_e-\omega)t + \frac{2\pi}{3} + \phi\right)\Re\left(\bar{Z}(\omega_e-\omega)\right)}{2|\bar{Z}(\omega_e-\omega)|^2} \\ &+ \alpha U_{AC} \frac{\sin\left((\omega_e-\omega)t + \frac{2\pi}{3} + \phi\right)\Im\left(\bar{Z}(\omega_e-\omega)\right)}{2|\bar{Z}(\omega_e-\omega)|^2} \\ &+ \alpha U_{AC} \frac{\cos\left((\omega_e+\omega)t + \frac{2\pi}{3} + \phi\right)\Re\left(\bar{Z}(\omega_e+\omega)\right)}{2|\bar{Z}(\omega_e+\omega)|^2} \\ &+ \alpha U_{AC} \frac{\sin\left((\omega_e+\omega)t + \frac{2\pi}{3} + \phi\right)\Im\left(\bar{Z}(\omega_e+\omega)\right)}{2|\bar{Z}(\omega_e+\omega)|^2} \\ &+ \alpha U_{DC} \frac{\cos\left(\omega_e t + \frac{2\pi}{3} + \phi\right)\Re\left(\bar{Z}(\omega_e)\right)}{|\bar{Z}(\omega_e)|^2} \\ &+ \alpha U_{DC} \frac{\sin\left(\omega_e t + \frac{2\pi}{3} + \phi\right)\Im\left(\bar{Z}(\omega_e)\right)}{|\bar{Z}(\omega_e)|^2} \end{aligned} \qquad (5)$$

With these definitions, I_{IN} can be computed by modulating back the three-phase currents to the DC side (I_{IN}). Indeed, I_{IN} is the image of the three-phase currents in the DC domain.

$$I_{IN} = I_a \alpha \cos(\omega_e t + \phi)$$

$$+I_b\alpha\cos\left(\omega_e t+\frac{2\pi}{3}+\phi\right)$$
$$+I_c\alpha\cos\left(\omega_e t-\frac{2\pi}{3}-\phi\right) \qquad (6)$$

It is also:

$$I_{IN}=\frac{3\alpha^2}{4}\frac{\Re\left(\bar{Z}(\omega_e-\omega)\right)}{|\bar{Z}(\omega_e-\omega)|^2}U_{AC}\cos(\omega t)$$
$$-\frac{3\alpha^2}{4}\frac{\Im\left(\bar{Z}(\omega_e-\omega)\right)}{|\bar{Z}(\omega_e-\omega)|^2}U_{AC}\sin(\omega t)$$
$$+\frac{3\alpha^2}{4}\frac{\Re\left(\bar{Z}(\omega_e+\omega)\right)}{|\bar{Z}(\omega_e+\omega)|^2}U_{AC}\cos(\omega t)$$
$$+\frac{3\alpha^2}{4}\frac{\Im\left(\bar{Z}(\omega_e+\omega)\right)}{|\bar{Z}(\omega_e+\omega)|^2}U_{AC}\sin(\omega t) \qquad (7)$$

The U_{DC} term of U_{IN} is dropped to ease the readability. It does not have any impact as U_{DC} is the AC part, U_{AC}, when $\omega\to 0$.

In phasor notation, $U_{AC}\cos(\omega t)$, $U_{AC}\sin(\omega t)$ and I_{IN} are:

$$\overline{U_{AC}\cos(\omega t)}=U_{AC}$$
$$\overline{U_{AC}\sin(\omega t)}=-jU_{AC}$$

$$\bar{I}_{IN}=\frac{3\alpha^2U_{AC}}{4}\left(\frac{\Re\left(\bar{Z}(\omega_e-\omega)\right)}{|\bar{Z}(\omega_e-\omega)|^2}+j\frac{\Im\left(\bar{Z}(\omega_e-\omega)\right)}{|\bar{Z}(\omega_e-\omega)|^2}\right)$$
$$+\frac{3\alpha^2U_{AC}}{4}\left(\frac{\Re\left(\bar{Z}(\omega_e+\omega)\right)}{|\bar{Z}(\omega_e+\omega)|^2}-j\frac{\Im\left(\bar{Z}(\omega_e+\omega)\right)}{|\bar{Z}(\omega_e+\omega)|^2}\right)$$
$$=\frac{3\alpha^2U_{AC}}{4}\left(\frac{1}{\bar{Z}^*(\omega_e-\omega)}+\frac{1}{\bar{Z}(\omega_e+\omega)}\right)$$

with $(A)^*$, the complex conjugate of complex number A.

Finally, the ratio between $\bar{U}_{IN}$ and $\bar{I}_{IN}$ gives the input impedance value:

$$\bar{Z}_{IN}(\omega)=\frac{\bar{U}_{IN}}{\bar{I}_{IN}}=\frac{U_{AC}}{\bar{I}_{IN}}$$
$$=\frac{4}{3\alpha^2}\left(\frac{1}{\bar{Z}^*(\omega_e-\omega)}+\frac{1}{\bar{Z}(\omega_e+\omega)}\right)^{-1} \qquad (8)$$

The equivalent impedance, as seen from the DC side, is composed out of two impedances **placed in parallel**. These impedances are the AC-side impedances located around the frequency of the PWM reference signal, ω_e.

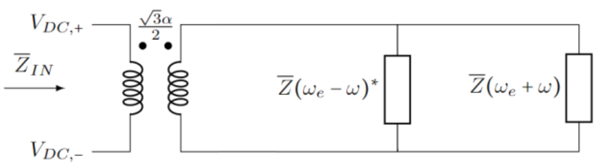

Figure 3:Schematic representation of Z_{IN}

CIRCUIT MODELING OF THE DC EQUIVALENT IMPEDANCE

In this section, an electrical model for the DC equivalent impedance is developed. The aim is to find an equivalent DC impedance circuit of the inverter associated to its AC impedance corresponding to (8), which has the frequency behaviour shown in Fig. 5. Important features of the frequency behaviour are extracted (pseudo resonant frequency, e.g.) and linked to the proposed electrical circuit target. The mapping is made using (8) and the transfer function of the suggested electrical DC impedance model (9).

This paper focuses on the circuit modeling of a general resistive and inductive load connected on the AC side of the AC/DC inverter/rectifier component (Fig.4).

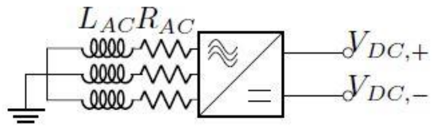

Figure 4: Circuit studied

Therefore, the equivalent impedance as seen from the DC side is:

$$\bar{Z}_{IN}(\omega)=\frac{1}{\alpha^2}\frac{2}{3R_{AC}}\frac{\omega_e^2L_{AC}^2+R_{AC}^2+j\omega 2R_{AC}L_{AC}+(j\omega)^2L_{AC}^2}{1+j\omega\frac{L_{AC}}{R_{AC}}}$$

Fig.5 represents the frequency behaviour of (8) with $\bar{Z}(\omega)=R_{AC}+j\omega L_{AC}$ (Fig. 4). The impedance exhibits a resonant effect around ω_e.Therefore, the suggestion is to create a DC equivalent impedance based on an RLC circuit (Fig.6).

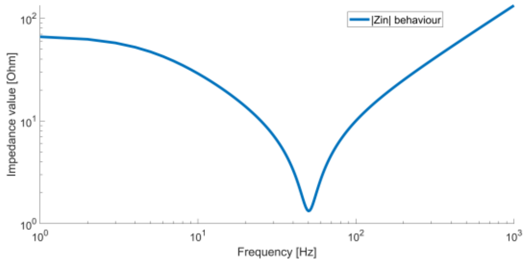

Figure 5: Impedance behaviour from (8)

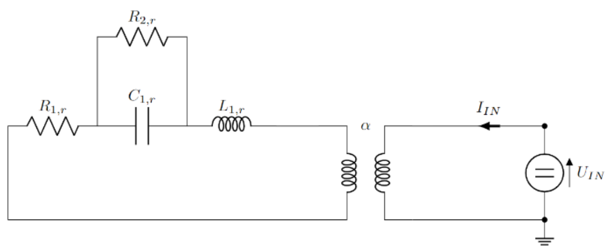

Figure 6: Electrical model proposed

The circuit depicted in Fig.6 is chosen with:

- $C_{1,r}$: the equivalent resonant capacitor
- $L_{1,r}$: the equivalent resonant inductor
- $R_{2,r}$: the constant effect at low frequencies
- $R_{1,r}$: the damping resistor of the equivalent resonant effect

The equivalent impedance of this model is:

$$\bar{Z}_{tot}(s=j\omega)=\frac{R_{1,r}+R_{2,r}+s\left(L_{1,r}+R_{1,r}R_{2,r}C_{1,r}\right)+s^2\left(R_{2,r}L_{1,r}C_{1,r}\right)}{1+sC_{1,r}R_{2,r}} \qquad (9)$$

Mapping $\bar{Z}_{IN}$ and $\bar{Z}_{tot}$ leads to:

$$C_{1,r}R_{2,r} = \frac{L_{AC}}{R_{AC}}$$

$$R_{1,r} + R_{2,r} = \frac{2}{3}\left(\frac{\omega_e^2 L_{AC}^2 + R_{AC}^2}{R_{AC}}\right)$$

$$C_{1,r}R_{1,r}R_{2,r} + L_{1,r} = \frac{4}{3}L_{AC}$$

$$C_{1,r}\,L_{1,r}R_{2,r} = \frac{2}{3}\frac{L_{AC}^2}{R_{AC}}$$

Solving these four equations with four unknowns, each model parameter of (9) is found:

$$R_{1,r} = \frac{2}{3}R_{AC}$$

$$L_{1,r} = \frac{2}{3}L_{AC}$$

$$C_{1,r} = \frac{3}{2}\frac{1}{L_{AC}\omega_e^2}$$

$$R_{2,r} = \frac{2}{3}\frac{\omega_e^2 L_{AC}^2}{R_{AC}}$$

In Fig.7, $|Z_{IN}(\omega)|$ and $|\bar{Z}_{tot}(j\omega)|$ are compared. The electrical model is close to the mathematical expression developed in the previous section.

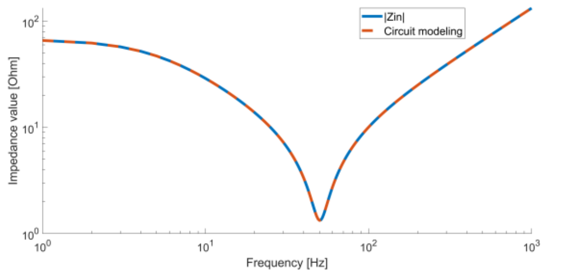

Figure 7: Comparison between the mathematical and electrical model of the impedance

RESULTS

Simulation

An EMT simulation has been carried out in order to verify the mathematical model developed in the second section. This simulation is done on MATLAB/Simulink software as shown in Fig.8. From this experiment, the DC current values are extracted and are visible in Fig. 9. It shows the accuracy of the complete mathematical model used to represent the electrical model developed in the previous section. These current values are directly measured on the DC side of the model as shown in Fig.8. The simulation focused on AC impedance (being representative of most LV grid connections).

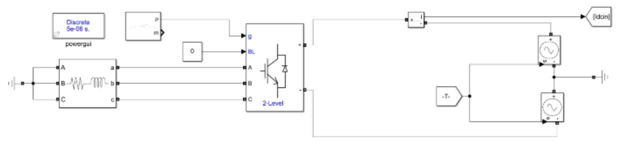

Figure 8: Simulated circuit in MATLAB/Simulink

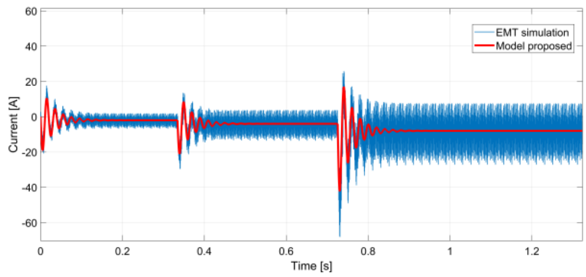

Figure 9: DC currents obtained from the simulation

In the previous figure, the red curve is the DC current provided by the model developed in this work. The blue curve is the switching model (the PWM is visible on the graph). The red curve is giving the mean value of the switching model as expected.

Experiment

In this section, an experiment is made to validate the mathematical model and the simulations made on MATLAB/Simulink. The experimental set-up is shown in Fig. 10.

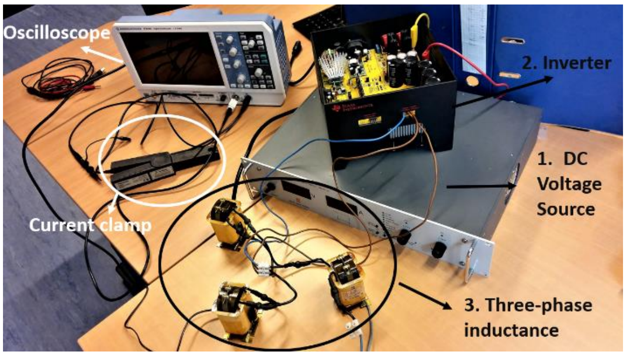

Figure 10: Experimental set-up (the measurement tools are in white and the circuit components in black)

Each numbered component, from Fig. 10, is:

1) A SM70 - 22 Power Supply (Delta Elektronika) [4]
2) A Texas Instrument Kit: High Voltage Motor Control and PFC Developer's Kit [5]
3) A X5011 Reactor Coil (Yaskawa) [6]

Based on this set-up, it is possible to evaluate R_{AC} and L_{AC} (Fig. 4) of the system shown in Fig.10.
The estimated resistance of the system is:

$$R_{AC} = 45.45\ 10^{-3} + 2 \cdot 7\ 10^{-3} + \mathbf{0.25} = 309.45\ \text{m}\Omega$$

This value is composed of several values:

- The measured value from a DC measurement
- The estimated value of the cables used to connect the inductance to the inverter [7]
- The factor 2 to take into account both sides of the inductance (primary and secondary)
- The resistance value ($\boldsymbol{R_{ds}}$) of the transistor inside the inverter [8]

The inductance is equal to the value indicated [6].

$$L_{AC} = 1\ mH$$

The circuit used for the experiment is shown in Fig. 11. C_{DC} is added to be the most representative to the inverter used as shown in the schematic in [5].

$$C_{DC} = 1650\ \mu F$$

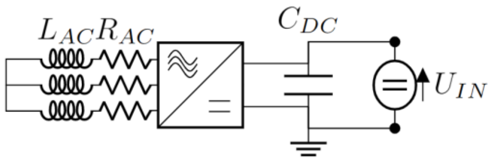

Figure 11: Circuit schematic of the experimental set-up

The experiment consists in a 1 Volt step voltage on U_{IN}. A mechanical switch is closed at the starting time of the experiment. The results are reported in Fig.12. The phase current and the current on the DC side of the converter are measured (brown and blue lines). The red curve is the current on the DC side computed using the proposed model. The DC current is measured experimentally with the set-up shown in Fig.10.

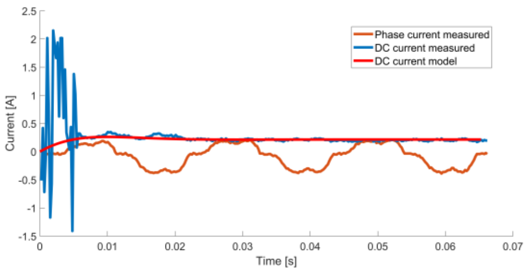

Figure 12: Experimental results

The DC model curve (coming from the theoretical part) is close to the DC current measured (experimental curve) as illustrated in Fig.12. The transient behaviour is well represented by the mathematical model. However, there is a difference between the mathematical model and the measurements at the beginning of the transient behaviour. With real devices, this difference can come from the estimated parameters (parasitic elements of the real circuit as capacitive effects e.g.) increasing the difference between the mathematical model and the experiment. However, after this "in-rush" current, the theoretical model is validated by the experimental results.

CONCLUSION

In this paper, an electrical model has been proposed considering the impact of the three-phase impedance on the DC side of a three-phase inverter. The mathematical development was shown along with the electrical model development. Next to these developments, results showing the accuracy of the model are demonstrated: a simulation on MATLAB/Simulink and a laboratory experimental validation. The general electrical model consists in a resonance passive circuit. The elements of the model depend on PWM parameters (modulating index, e.g.). Therefore, the outer loop control does not have any impact on the behaviour of the model developed. However, the system modeled does not involve any active components (e.g. voltage sources). In a future work, the modeling of active components will be done to represent the AC side of the inverter in a more realistic way. A control design will also be studied using the model proposed in this work. It is part of a future work concerning the DC modeling of the grid impedance through an inverter.

REFERENCES

[1] Schiltz, N. (2016) Tesla v. Edison: War of currents part I, Grace Technologies_FC. Available at: https://www.graceport.com/blog/tesla-v-edison-war-of-currents-part-i (Accessed: December 14, 2022).

[2] DC microgrids (no date) Microgrid Projects. Available at: http://microgridprojects.com/dc-microgrids/ (Accessed: December 14, 2022).

[3] P. Mattavelli et al., Generators and loads models to investigate uncontrolled islanding on active distribution networks, CIRED 2015, Lyon, paper 0780

[4] ROOD, "SM70-22," cnrood.com, https://www.cnrood.com/en/sm70-22 (accessed on August 02, 2022).

[5] Texas Instrument, "TMDSHVMTRPFCKIT High Voltage Motor Control and PFC Developer's Kit," ti.com, https://www.ti.com/product/TMDSHVMTRPFCKIT/partdetails/TMDSHVMTRPFCKIT (accessed on August 02, 2022).

[6] TeamEquip, "Yaskawa X5011 Reactor Coil 8 A, 1 mH T32245," teamequip.com, https://teamequip.com/yaskawa-x5011-reactor-coil-8-a-1-mh-t32245/ (accessed on August 02, 2022).

[7] RS, "Fiche banane 4 mm Schutzinger Vert Mâle 16A 33 V ac, 70V c.c.," fr.rs-online.com, https://fr.rs-online.com/web/p/fiches-bananes/1796754 (accessed on August 02, 2022).

[8] Infineon, "CoolMOS™Power Transistor," IPP60R250CP, 2012-01-05.